Journal of Materials Chemistry B

Accepted Manuscript

ROYAL SOCIETY OF CHEMISTRY

www.rsc.org/materialsB

Journal Name

RSCPublishing

ARTICLE

Co-immobilization of enzymes with the help of a dendronized polymer and mesoporous silica nanoparticles

Cite this: DOI: 10.1039/x0xx00000x

Received 00th January 2012,
Accepted 00th January 2012

DOI: 10.1039/x0xx00000x

www.rsc.org/

Hanna Gustafsson[§a], Andreas Küchler[§b], Krister Holmberg[a] and Peter Walde[b*]

The two enzymes *Aspergillus* sp. glucose oxidase (GOD) and horseradish peroxidase (HRP) were co-immobilized on solid silica supports in a spatially controlled way by using mesoporous silica nanoparticles (Hiroshima Mesoporous Materials, HMM) and a polycationic dendronized polymer (denpol). The silica support was first coated with the denpol, followed by the deposition of the mesoporous silica nanoparticles into which – in a next step – GOD was adsorbed. Finally, the GOD-loaded silica nanoparticles were coated with a denpol-HRP conjugate constituting of several HRP molecules which were covalently bound to the denpol *via* bis-aryl hydrazone (BAH) bonds. The entire immobilization process was followed in real time with quartz crystal microbalance with dissipation monitoring (QCM-D). The activities and storage stabilities of the co-immobilized enzymes were determined by analyzing a two-step cascade reaction involving the two immobilized enzymes GOD and HRP. D-glucose and *o*-phenylenediamine (OPD) were used as substrates for GOD and HRP, respectively. The cascade reaction – in which intermediate hydrogen peroxide was formed from D-glucose and dissolved O_2 with GOD – was shown to take place. The immobilized enzymes remained fairly stable for at least 2 weeks if stored in contact with an aqueous solution of pH = 7 at 4 °C. If, however, denpol-BAH-GOD coated HRP-loaded mesoporous silica nanoparticles were used (the reversed situation), the cascade reaction was not effective. This was probably due to slow diffusion of hydrogen peroxide from the surface-exposed GOD to the particle-trapped HRP, and/or due to an inefficient loading of active HRP inside the particles. Overall, the combination of two enzyme immobilization methodologies – enzymes adsorbed within mesoporous silica nanoparticles and enzymes adsorbed as denpol-BAH-enzyme conjugates – allows the spatially controlled localization of different types of enzymes in a simple way. Possible applications of the concept are in the field of bioelectrode fabrication.

Introduction

Enzyme immobilization is a straightforward method that enables recycling of enzymes, improvement of the enzyme stability and enhancement of product recovery.[1-10] Development of co-immobilized multi-enzymatic systems is highly interesting from an environmental and economic point of view.[11-15] Through co-immobilization it is possible to perform a one-pot reaction instead of isolated steps and thereby the accumulation of undesired intermediates and byproducts can be avoided. An enzymatic cascade reaction may also proceed in a highly chemo- or stereoselective way compared to a conventional organic synthesis process, resulting in more well-defined end products.[16] Moreover, the loss of unstable intermediates can be reduced through *in situ* generation of substrates.[17] Immobilized multi-enzyme systems can also be utilized in biosensors for the quantification of molecules of biological interest, like D-glucose.[18]

In previous investigations from our two groups we have used two different approaches for the immobilization of enzymes: (i) immobilization in mesoporous silica nanoparticles, and (ii) immobilization onto silica surfaces with the help of a

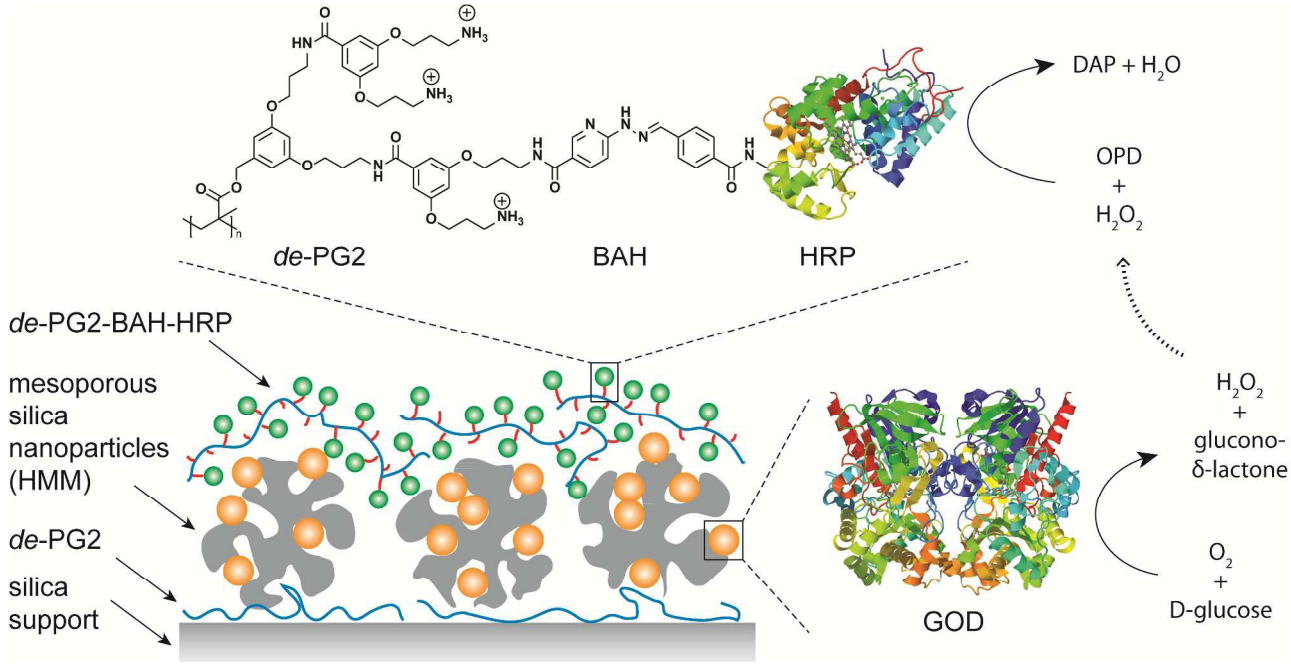

Scheme 1. An illustration of the co-immobilized system prepared in a way resembling the layer-by-layer methodology. The first layer is formed by the denpol *de*-PG2, the second by GOD-loaded mesoporous silica nanoparticles, and the third by the *de*-PG2-BAH-HRP conjugate. In this way, a spatially controlled localization of the two enzymes on a solid silica support can be achieved. The two enzymes catalyze a sequential cascade reaction: GOD oxidizes D-glucose with dissolved dioxygen, yielding glucono-δ-lactone and hydrogen peroxide, which serves as oxidizing agent for the HRP catalyzed oxidation of OPD (*o*-phenylenediamine) yielding DAP (2,3-diaminophenazine). GOD: glucose oxidase, PDB code 3QVP; HRP: horseradish peroxidase (isoenzyme C), PDB code 1H5A; BAH: bis-aryl hydrazone. Please note that the carbohydrates on the surface of the two glycosylated enzymes are not shown.

dendronized polymer. In the *first approach*, different types of mesoporous silica nanoparticles were used as support for enzymes.[19-23] Enzyme immobilization occurred through physical adsorption in the pores and, to a minor extent, onto the particle's outer surface. The porous structure has the advantage of providing a very large surface area, which allows for a high enzyme loading.[2, 7, 24-27] In the *second approach*, enzyme immobilization on flat silica surfaces, *i.e.* onto microscopy glass slides and glass coverslips, or inside glass micropipettes, was achieved by using a polycationic second generation dendronized polymer (denpol), abbreviated as *de*-PG2 (see Scheme 1).[28, 29] The prefix "*de*" indicates that in the denpol *de*-PG2 the protecting group used during the denpol synthesis (*tert*-butyloxycarbonyl) was no more present; *de*-PG2 is a *deprotected* denpol.[30, 31] In the most recent work, the enzymes were first covalently linked to *de*-PG2 along the denpol chain *via* bis-aryl hydrazone (BAH) bonds, whereby *de*-PG2-BAH-enzyme conjugates were obtained which were subsequently adsorbed onto silica surfaces.[28] Due to the polycationic nature of the denpol and due to the fact that several enzymes were linked to the polymer chain, binding of the conjugate to glass surfaces could be achieved efficiently *via* multiple interactions.

In the present work we present a method for the spatially controlled co-immobilization of two different types of enzymes, horseradish peroxidase (HRP) and *Aspergillus* sp. glucose oxidase (GOD), by *combining the two approaches*. GOD and HRP serve as model enzymes which catalyze two steps of an enzymatic cascade reaction. Scheme 1 depicts the entire system, which was prepared stepwise in a way which resembles the layer-by-layer methodology.[32-37] Borosilicate glass was used as support and the first layer was formed by *de*-PG2, which was used in the first step as a "primer", *i.e.* as binding layer. The second layer consisted of GOD-loaded mesoporous silica nanoparticles, and the third one was the *de*-PG2-BAH-HRP conjugate. The combination of the two techniques enabled the preparation of a system with enzymes in a controlled arrangement to each other. In order to find out whether the relative location of the two enzymes is essential for the cascade reaction to take place, a reversed system was also prepared, with HRP immobilized in the mesoporous nanoparticles and with GOD covalently linked to the denpol (*de*-PG2-BAH-GOD) and added onto the immobilized particles. Quartz crystal microbalance with dissipation monitoring (QCM-D) has previously been shown to be a simple and robust measuring technique for real time studies of enzyme immobilization in mesoporous silica particles.[23] Here we demonstrate the complete co-immobilization process in real time with QCM-D. We also evaluated the efficiency of the cascade reaction and the stability of the system.

Materials and methods

Chemicals and enzymes

NaH_2PO_4, NaCl, aminopropyltrimethoxysilane (APTMS), *o*-phenylenediamine (OPD), and D-glucose were all purchased from Sigma-Aldrich. 2,2'-Azino-bis(3-ethylbenzothiazoline 6-

sulfonic acid) diammonium salt ($ABTS^{2-}(NH_4^+)_2$) was obtained from Fluka (Switzerland). The non-porous silica nanoparticles (Bindzil 50/80) were a gift from AkzoNobel Pulp and Performance Chemicals AB (Bohus, Sweden). The sodium phosphate buffers (PBS, pH 5 -7) were prepared to 10 mM concentrations with 150 mM NaCl and the pH adjusted with NaOH. Glucose oxidase from *Aspergillus* sp. (GOD, product GLO-2022, Lot 9448520002, 242 U/mg, EC 1.1.3.4, M ≈ 153 kDa) and horseradish peroxidase isoenzyme C (HRP, product PEO-131, grade I, lot 2131616000, 278 U/mg, EC 1.11.1.7, *M* ≈ 44 kDa) were purchased from Toyobo Co. Ltd., Japan, obtained through Sorachim SA, Switzerland. Protein concentrations were determined by UV/VIS spectrophotometry using the molar absorption coefficients $\varepsilon_{280nm}=2.7\cdot10^5$ $M^{-1}\cdot cm^{-1}$ [38] and $\varepsilon_{450nm}=2.82\cdot10^4$ $M^{-1}\cdot cm^{-1}$ [39] for GOD and $\varepsilon_{403nm}=1.02\cdot10^5$ $M^{-1}\cdot cm^{-1}$ for HRP.[40] The glass coverslips (borosilicate, round, #1.5, 8 mm diameter) were obtained from Science Services, Germany. Enzyme stock solutions were prepared in either pH 5 or pH 6 buffer solution. Prior to the immobilization, the enzyme solutions were "washed" with pH 5 or pH 6 buffer using spin filters (Amicon Ultra – 4 ml 10 K ultracel).

Mesoporous silica nanoparticles and dendronized polymers

The mesoporous silica nanoparticles used as support for GOD (or HRP) immobilization were spherical with a diameter around 40 nm and with a pore size around 9 nm (abbreviated as HMM, Hiroshima Mesoporous Materials), see Figure 1. For the synthesis and characterization of the particles, the reader is referred to our previously published work;[19] the synthesis protocol was adapted from Nandiyanto *et al.*[41] Transmission electron microscopy (TEM) was performed with a FEI Tecnai T20 LaB6 transmission electron microscope operated at 200 kV. The samples were prepared by grinding and dispersing the particles in ethanol, put in an ultrasonic bath and deposited onto a holey carbon-coated copper grid. The ethanol was subsequently evaporated. Scanning electron microscopy (SEM) was performed with a Leo Ultra 55 FEG scanning electron microscope operated at 2 kV and a working distance of 1.7-2.2 mm.

The denpol used was the same as the one applied by Küchler *et al.*,[28] a polycationic second generation denpol (*de*-PG2), synthesized as described previously,[30] with P_n=1400 (*i.e.* number averaged repeating units per chain, r.u. = 1400) and PDI=4.74, previously abbreviated as *de*-$PG2_{1400}$.[28]

Dendronized polymer-enzyme conjugates

The denpol-BAH-enzyme conjugate *de*-PG2-BAH-HRP was synthesized as described by Grotzky *et al.*,[42] with small modifications.[28] In short, about 5 % of the peripheral amino groups of the dendronized polymer were functionalized with 6-hydrazinonicotinamide acetone hydrazone. HRP was functionalized with a 4-formylbenzamide moiety with an average modification ratio of 0.85 linkers per HRP. The conjugation of functionalized polymer and HRP was carried out using 10 mM aniline as a catalyst.[43] For further details, including the synthesis of *de*-PG2-BAH-GOD, see Küchler *et al.*[28] On average, a 1400 r.u. long *de*-PG2-BAH-HRP conjugate had about 108 HRP molecules (abbreviated as *de*-$PG2_{1400}$-BAH-HRP_{108}), and it was estimated that a 1400 r.u. long *de*-PG2-BAH-GOD conjugate carried approximately 50 GOD molecules (abbreviated as *de*-$PG2_{1400}$-BAH-$GOD_{\approx50}$).[28]

Studying the enzyme immobilization process with QCM-D

Immobilization of GOD (or HRP) in mesoporous silica nanoparticles (HMM) was followed in real time using QCM-D. The technique is capable of measuring mass changes in the nanogram range while at the same time monitoring the viscoelastic properties when molecules dissolved in a liquid adsorb to the sensor surface. The adsorbed mass is related to changes in resonance frequency and the viscoelastic properties are related to changes in dissipation. Dissipation is detected as damping or decay of vibrations in the film adsorbed to the sensor, thus softer and more flexible films result in increased dissipation. More details about QCM-D can be found elsewhere.[44] The QCM-D experiments were run on a Q-Sense E4 instrument equipped with a QAFC 301 axial flow chamber (Q-Sense AB, Gothenburg, Sweden). Cleaning of the silicon dioxide (SiO_2) coated sensors (QSX 303, Q-Sense) was performed according to our previously published protocol.[23]

The immobilization of either HRP or GOD in the mesoporous silica nanoparticles was performed in PBS at pH 5 and pH 6 in order to find the optimal conditions for each of the two enzymes. Comparison was also made with the adsorption on non-porous particles. For these measurements, both the porous and the non-porous nanoparticles were attached to the QCM-D sensor using aminopropyltrimethoxysilane (APTMS) as a linker. The silanization protocol was based on previous work.[23] The APTMS-functionalized sensors were mounted into the QCM-D chamber and a suspension of 0.4 % (w/v) of silica particles in 0.01 M HCl was flowed (25 µl/min, 21º C) through the system. The subsequent enzyme immobilization was performed using enzyme solutions of pH 5 or 6. For the enzyme loadings to be comparable, the data were normalized according to frequency shifts during the binding of silica nanoparticles to the sensor. At least three measurements were performed and all frequency shifts presented are based on data recorded at the 5th overtone. The particle distribution on the QCM-D sensor was studied with SEM.

For the co-immobilization of GOD and HRP cleaned silicon dioxide coated QCM-D sensors were mounted into the QCM-D chamber and a *de*-PG2 solution (20 µM r.u., pH 5) was flowed through the system (25 µl/min, 21ºC). In the subsequent steps, the sensors were exposed to a suspension of 0.4 % (w/v) mesoporous silica particles (pH 5), followed by a 2 µM GOD solution (pH 5) and thereafter a 7.5 µM (r.u.) solution of HRP conjugated with *de*-PG2 (*de*-PG2-BAH-HRP). For optimal performance, the denpol-enzyme conjugate was in pH 7 PBS. The same buffers used for the adsorption of *de*-PG2, the silica particles, GOD, and *de*-PG2-BAH-HRP were also flowed through the chambers in-between the individual adsorption steps to wash away residual material.

For the reverse enzyme co-immobilization, a 10 µM HRP solution (pH 5) was added to the adsorbed mesoporous silica particles, followed by addition of a solution of *de*-PG-BAH-GOD (about 14 µM r.u., pH 5).

Enzyme immobilization on glass coverslips and analysis of the activity of the immobilized enzymes

For the enzymatic activity assays, microscopy glass coverslips with 1 cm^2 surface were first cleaned 3 times in ethanol in a sonication bath and subsequently submitted to oxygen plasma treatment for 2 min (Plasma Cleaner/Sterilizer PDC-32G, Harrick). For storage, the cleaned coverslips were immersed in adsorption buffer (PBS pH 5) in a 2 mL polypropylene reaction tube immediately after the plasma treatment. Deposition of the adsorbed layers on the surface was performed according to the optimal conditions elaborated with the QCM-D measurements. After each adsorption step, the coverslips were washed 3 times with the corresponding adsorption buffer (pH 5, except for the *de*-PG2-BAH-HRP conjugate which was used at pH 7) to remove residual solute from the reaction tubes. The first layer consisting of *de*-PG2 was adsorbed by immersing the coverslips in a *de*-PG2 solution for 1 h (concentration of repeating unit 20 µM in adsorption buffer pH 5). After washing, the coverslips were kept in the adsorption buffer (pH 5) for 1 h before further adsorption steps were carried out. Adsorption of the HMM particles was performed by immersion of the denpol-coated coverslips in a 0.4 % (w/v) particle suspension in adsorption buffer pH 5. Subsequent GOD loading was performed by 1 h incubation in a 2 µM GOD solution (pH 5). Adsorption of *de*-PG2-BAH-HRP was performed overnight in a 7.5 µM solution (r.u. concentration, pH 7). For the reverse enzyme co-immobilization, the coverslips containing adsorbed particles were incubated with a 10 µM HRP solution (pH 5), followed by incubation with a solution of *de*-PG2-BAH-GOD (about 14 µM r.u., pH 5).

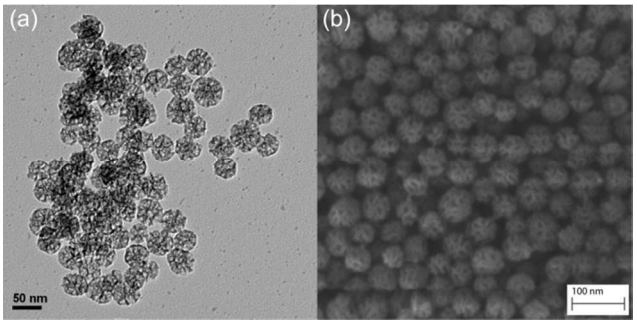

Figure 1. TEM (a) and SEM (b) images of the HMM (silica nanoparticles) used, with a particle diameter of around 40 nm.

The enzymatic activity of HRP was quantified using $ABTS^{2-}$ as a chromogenic substrate and hydrogen peroxide as electron acceptor.[45] Product formation was monitored with a Specord S600 spectrophotometer and quantified using the absorption band at 414 nm (ε_{414nm} ($ABTS^{\bullet-}$) = 36000 $M^{-1}\cdot cm^{-1}$).[45] A calibration curve was measured using known concentrations of HRP in solution.[28] For activity measurements, the glass coverslips were immersed in 1 mL of substrate solution (1 mM $ABTS^{2-}$, 200 µM H_2O_2, PBS pH 7), and the reaction tube was agitated gently by inverting it two to three times. The reaction mixture was analyzed spectrophotometrically with disposable polystyrene cuvettes of 1 cm path length after a defined time (Figure S1, ESI) and the apparent enzyme concentration was read from the calibration curve.[28]

For low HRP concentrations, as encountered in the case of HRP immobilized in adsorbed HMM particles, an alternative assay − which allowed elongated incubation times − was applied: 3.14 mM OPD (*o*-phenylenediamine) was used as a chromogenic substrate in PBS pH 7, and 80 µM H_2O_2 was added as oxidant. The formation of the product DAP (2,3-diaminophenazine) was followed spectrophotometrically at 418 nm (Figure S2, ESI; ε_{418nm} (DAP) = 16700 $M^{-1}\cdot cm^{-1}$).[46] Quantification of the apparent HRP concentration was performed in a similar way as described for the $ABTS^{2-}$-based assay, but using an appropriate calibration curve made with OPD.[47]

The GOD activity was quantified using a combined assay including 3.45 mM D-glucose and dissolved dioxygen (as available in non-degassed buffer) as substrates and 2 nM HRP and 3.14 mM OPD for *in situ* detection of the hydrogen peroxide formed.[29] The assay was performed in PBS pH 7 and a calibration curve was recorded with known concentrations of GOD.[28] 1 mL of premixed assay solution was added to the glass coverslips in a reaction tube and agitated gently by inversion. After a defined time, UV/VIS spectra of the assay solution were recorded and the formation of DAP was quantified (Figure S3, ESI).

For the analysis of the cascade reaction catalyzed by the two immobilized enzymes, GOD and HRP, the same reaction mixture as for the GOD analysis was used, but the addition of HRP in solution was omitted (Figure S4, ESI).

All activity assays were run in 1 mL of substrate solution and with a glass coverslip with 1 cm^2 surface; all assays were performed in triplicates. Mean values and standard deviations are given. As mentioned above, for both enzymes, quantification of the amount of immobilized enzyme was based on a comparison of the activities of the immobilized enzymes with the activities of the enzymes in bulk solution. It was assumed that the immobilized enzymes have the same kinetic properties as the free enzymes in solution. With this

assumption, the apparent enzyme concentrations could be converted to apparent enzyme coverage per square centimeter, *i.e.* an activity of immobilized enzyme corresponding to 1 nM enzyme in bulk corresponded to 1 pmol enzyme/cm^2 (1 nM = 10^{-12} mol/mL; 1 cm^2 surface per mL).

Results and discussion

QCM-D studies of the immobilization of HRP or GOD in mesoporous silica nanoparticles

In order to monitor enzyme immobilization in porous and on non-porous silica particles with the QCM-D technique, the particles were first attached to a silica coated sensor. For the particles to bind, a silane linker containing an amino group (APTMS, aminopropyltrimethoxysilane) was grafted onto the silica-coated sensor leading to an amino-terminated surface.

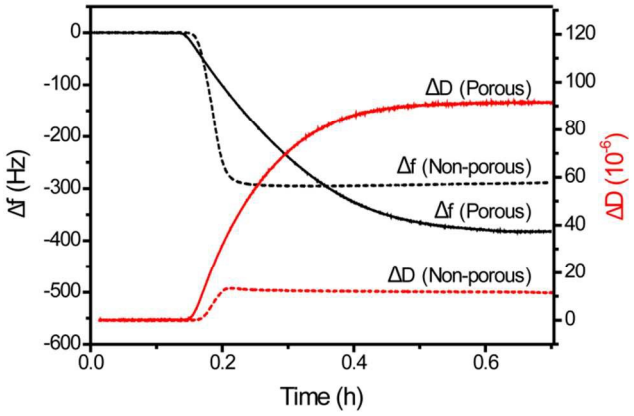

Figure 2. QCM-D results, presented as shift in frequency (Δf, black) and dissipation (ΔD, red) as a function of time, showing the attachment of silica nanoparticles onto an APTMS-coated sensor (pH 2).

The APTMS modified sensor was then mounted in the QCM-D chamber with a subsequent continuous flow of a HMM silica nanoparticle suspension (in 0.01 M HCl). During the particle adsorption, a significant negative frequency shift together with an increase in the dissipation was observed (Figure 2). This is an indication of adsorption of the negatively charged silica nanoparticles onto the positively charged sensor surface. For a detailed discussion of the particle adsorption results, the reader is referred to our previously published work.[23]

After successful attachment of the silica particles to the APTMS-coated sensor, either HRP or GOD dissolved in PBS (pH 5 or pH 6) was immobilized. The immobilized amount of HRP (M ≈ 44 kDa) was more than four times as large for the mesoporous nanoparticles at pH 6 than for the non-porous particles (Figure 3a). For the rather large GOD (M ≈ 153 kDa) the adsorbed amount at pH 6 was more than three times larger than in the case of the non-porous particles (Figure 3b). In addition, a lower enzyme *desorption* was observed for the porous particles (HRP ~7 %, GOD ~5 %) compared to the non-porous particles (HRP ~45 %, GOD ~20 %). This is a clear indication that in the case of the porous particles, the majority of the immobilized enzymes were located inside the pores and cavities and not on the external surface.

Since both the charge of the adsorbing enzyme and the potential of the silica surface vary with pH, electrostatic interactions between the enzyme and the support may be governed by the pH of the buffer. By decreasing the pH of the buffer from 6 to 5, the amount of immobilized HRP in the HMM nanoparticles increased significantly (Figure 3a). At the same time, the desorption decreased from ~7 % to ~4 %. The point of zero charge (pzc) for silica is 2-3[48] and the isoelectric point (pI) of HRP (isoenzyme C) is 8.8.[49] When decreasing the pH, HRP will become more positively charged leading to a stronger interaction with the negatively charged silica support, which is one of the factors contributing to a larger amount of immobilized HRP at pH 5 as compared to pH 6.

The decrease of the pH also resulted in an increased amount of

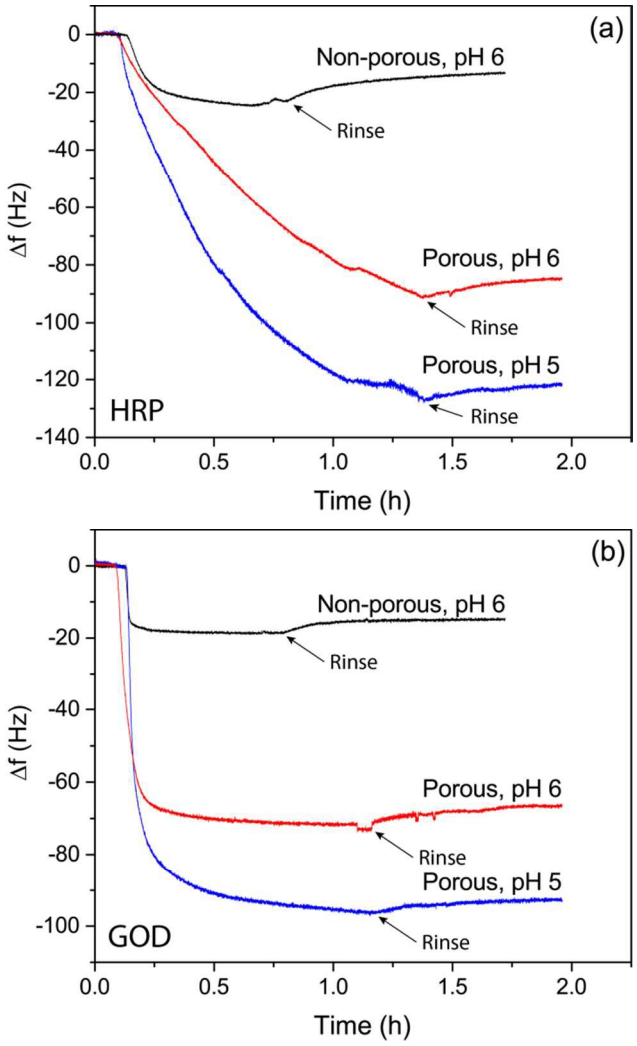

Figure 3. QCM-D results, presented as frequency shift (Δf) as a function of time, during the immobilization of (a) HRP and (b) GOD in mesoporous and on non-porous silica nanoparticles at pH 5 or pH 6. The immobilization was followed by a rinsing step.

immobilized GOD (Figure 3b) and a reduced desorption from ~5 % to ~2 %. At a pH above the pI of GOD (pI = 4.2)[50] both

the silica and the enzyme are negatively charged and by approaching the pI, the overall charge of GOD will become less negative, which means that the repulsive forces between the enzyme and the support will be diminished. However, positively charged surface areas of the enzyme can exist even though the overall charge is negative. Moreover, other interactions, such as hydrophobic interactions and hydrogen bonding, may also be involved during the immobilization, creating attractive interactions between enzyme and support.

To visualize the viscoelastic effect of the immobilized enzymes, the frequency shift (Δf) was plotted against the corresponding dissipation shift (ΔD) (Figure 4). The curves in these Δf *vs.* ΔD plots can be divided into different regimes, representing variations in the enzyme behavior during the adsorption. For the adsorption of HRP two regimes were

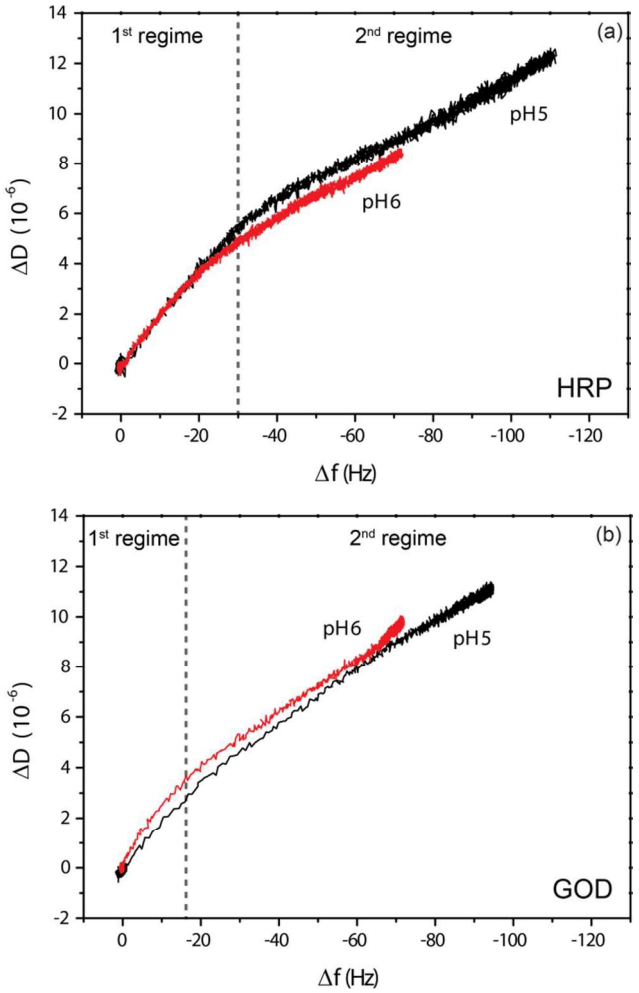

Figure 4. Dissipation (D) versus frequency shift (Δf) plot showing the dissipative behavior of the immobilized (a) HRP and (b) GOD in HMM.

observed. The first regime shows a large shift both in frequency and dissipation (Figure 4a). In the second regime the dissipation levels off with a continuing increase in frequency. The slower increase in dissipation in the second regime indicates that the HRP adsorption to the outer particle surface slowed down due to saturation whereas the diffusion into the pores continued. This division into two regimes is not as apparent for GOD, as can be seen in Figure 4b.

Overall, the immobilization of HRP or GOD in the mesoporous silica nanoparticles occurred most efficiently at pH 5. Therefore, for the following co-immobilization experiments, pH 5 buffer solutions were used.

QCM-D studies of the co-immobilization of HRP and GOD by use of mesoporous silica nanoparticles and the dendronized polymer *de*-PG2

For the co-immobilization of the two enzymes the denpol, *de*-PG2, was used as a bottom layer ("primer") instead of APTMS. As discussed below, the use of adsorbed *de*-PG2 as binding layer has advantages over conventional APMTS. On top of the denpol layer the mesoporous HMM nanoparticles were adsorbed, followed by either immobilization of HRP inside the particles and thereafter *de*-PG2-BAH-GOD (Figure 5a), or first GOD inside the particles and then *de*-PG2-BAH-HRP (Figure 5b and Scheme 1). During the polymer adsorption, a three-step change in frequency and dissipation was observed (Figure 5, and Figure S5, ESI). This stepwise change in frequency and dissipation can be explained by polymer rearrangements on the surface together with an uptake and release of solvent molecules (water). It is worth noting that with the denpol as bottom layer it is possible to adsorb a larger amount of HMM particles than with APTMS (compare the frequency change after addition of the HMM particles in Figure 2 and Figure 5, as well as the SEM images of the QCM-D sensor surfaces in Figure S6, ESI). This high efficiency of *de*-PG2 for adsorbing mesoporous silica particles is possibly due to the rough and larger surface the adsorbed denpol creates as compared to APTMS. Another possibility is that the denpol is more efficiently attached to the silica sensor than APTMS and does not leave any bare spots to which the particles are unable to bind. The change in dissipation (ΔD) is also smaller in this denpol system as compared to APTMS, which can be due to a tighter attachment of the particles to *de*-PG2 than to APTMS.

Surprisingly, however, the amount of HRP which adsorbed in the mesoporous silica nanoparticles was lower if *de*-PG2 was used as bottom layer as compared to APTMS (Figure 3a and Figure 5a), despite the lower amounts of adsorbed particles in the latter case. It is conceivable that the HMM particles were partly buried in the denpol layer, which could hinder access of the enzyme molecules to some of the particles. The final *de*-PG2-BAH-GOD layer was successfully adsorbed at pH 5 (Figure 5a). It is likely that the conjugate enfolded around the HMM particles.

The amount of GOD immobilized in the HMM particles was slightly larger with *de*-PG2 than with APTMS as bottom layer and was also larger compared to the amount of immobilized HRP. The larger amount of immobilized GOD compared to HRP was confirmed to be due to unspecific binding of the negatively charged GOD to the positively charged *de*-PG2 (data not shown). Up to this point, pH 5 buffer was used. However, the final step, *i.e.* the adsorption of *de*-PG2-BAH-HRP onto GOD-loaded HMM particles, proceeded poorly at pH 5. This

behavior was not observed when *de*-PG2-BAH-HRP was directly adsorbed to the HMM particles without immobilized GOD (data not shown). The pH was then increased to pH 7, which resulted in an efficient adsorption of *de*-PG2-BAH-HRP to the GOD-loaded HMM particles (Figure 5b). It is likely that the positive effect of the increase in pH is due to an increase of the negative charge on the GOD-loaded particle surface. At pH 5 the overall negative charge of GOD is quite low as its pI is 4.2.[50] The driving force for the adsorption of the positively charged *de*-PG2-BAH-HRP onto the GOD-loaded silica nanoparticles is likely to increase with increasing negative charge of the adsorbed particles.

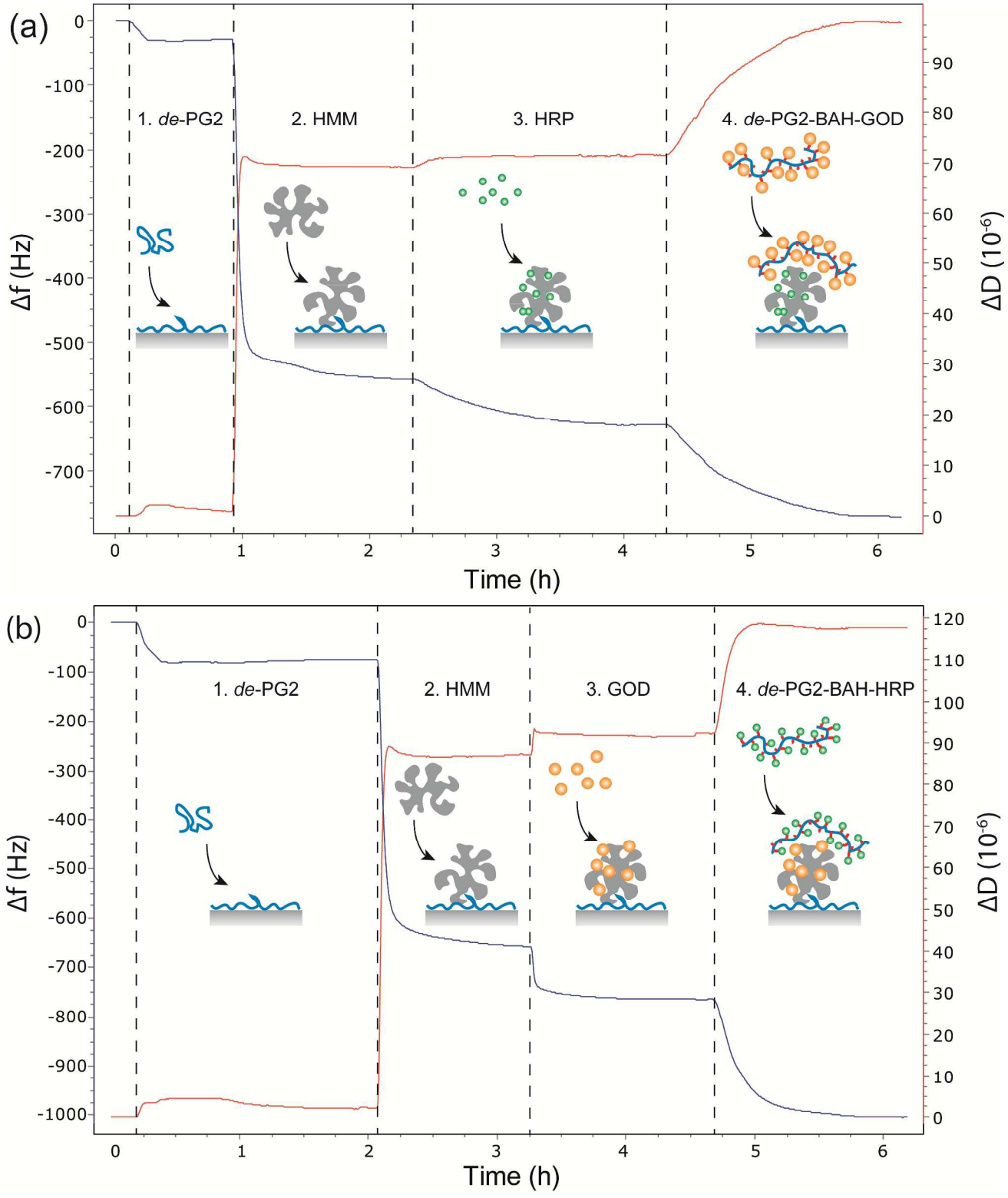

Figure 5. Frequency and dissipation curves for the co-immobilization of (a) HRP followed by GOD and (b) GOD followed by HRP. Step (1) represents adsorption of the polycationic denpol *de*-PG2 to a silica-coated sensor (pH 5), (2) attachment of porous silica nanoparticles onto the denpol (pH 5), (3) immobilization of the first type of enzyme (HRP or GOD) into the nanoparticles (pH 5), and (4) adsorption of the second type of enzyme, covalently linked to the denpol (*de*-PG2-BAH-GOD (pH 5) or *de*-PG2-BAH-HRP (pH 7)).

Activity and stability of the co-immobilized enzymes

The activity of immobilized HRP was measured at pH 7 with two different assays. Usually, the chromogenic substrate $ABTS^{2-}$ was used, which upon oxidation by HRP yields the radical chromophore $ABTS^{\bullet-}$ (Figure S1, ESI).[45] For low HRP activities, as encountered in the case of HRP immobilized inside the HMM silica particles, OPD was used instead of $ABTS^{2-}$.[47] The enzymatic oxidation of OPD and the subsequent dimerization leads to the formation of DAP (Scheme 1). This latter OPD/DAP system allows for elongated assay times, therefore giving low detection limits.[47] GOD activity measurements were performed by exploiting an enzymatic cascade reaction:[28] Oxidation of D-glucose by GOD using dissolved dioxygen (O_2) as the electron acceptor yields glucono-δ-lactone and hydrogen peroxide (H_2O_2) (Scheme 1). The latter can then be quantified in presence of an excess of HRP and OPD as chromogenic HRP substrate.[29] The activity of the immobilized enzymes was evaluated by analysis of the product formation upon immersion of glass coverslips (1 cm^2 surface coated with enzymes) into 1 mL assay solution. The resulting apparent amount of enzyme corresponds to the amount of substrate-accessible, active enzyme, see Materials and methods.

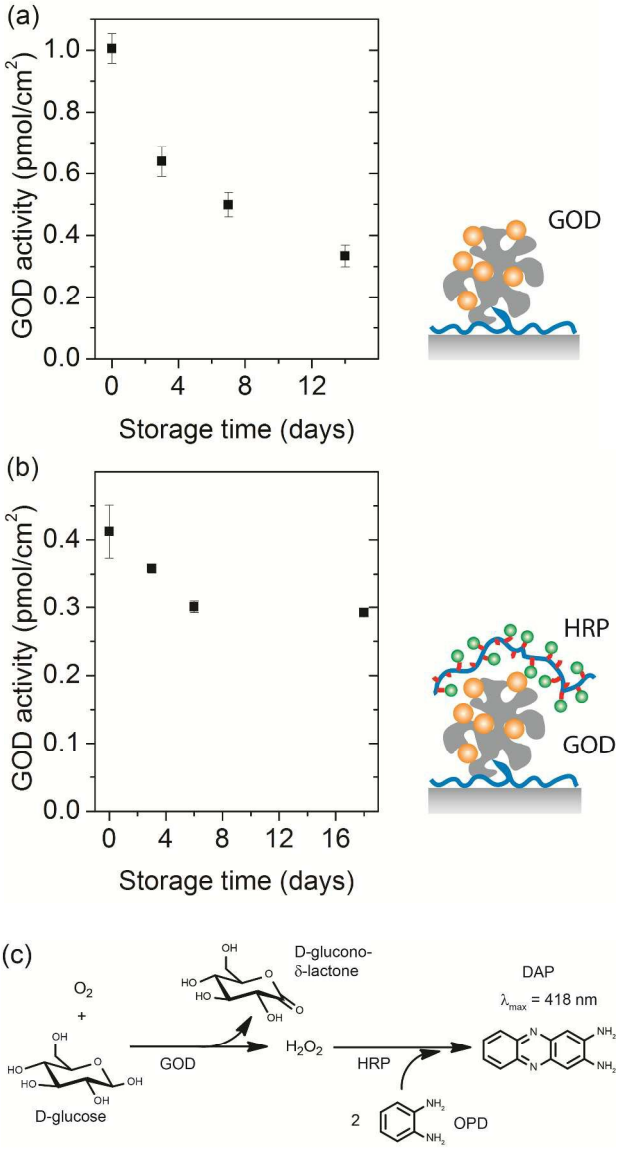

Figure 6. Apparent activity and stability of GOD immobilized in HMM nanoparticles attached on *de*-PG2-coated glass coverslips without any additional coating with a denpol layer (a), and with an additional layer of *de*-PG2-BAH-HRP (b). Since the activity of GOD in the latter case was measured *without* additional HRP in the assay mixture, the activity can be assigned entirely to the surface localized enzymatic cascade reaction. Storage temperature: 4 °C; PBS pH = 7. The reaction scheme of the enzymatic cascade reaction used for the activity measurements is given in (c). See materials and methods for details.

For a first series of activity and stability measurements, a layer of *de*-PG2 was deposited first on the glass surface, followed by adsorption of HMM nanoparticles. Subsequent loading of the particles with HRP resulted in a layer of HRP-loaded particles which was exposed to the pH 7 assay solution (without any further covering with a denpol layer). This layer exhibited a HRP activity corresponding to 0.05 pmol HRP/cm^2. Upon covering these HRP loaded HMM particles with *de*-PG2-BAH-GOD, the HRP activity decreased, corresponding to 0.03 pmol HRP/cm^2, while the determined GOD activity corresponded to a GOD coverage of 0.9 pmol GOD/cm^2. Different features of the covering layer can be considered to contribute to the reduction in HRP activity, such as a slower diffusion of the substrate from the bulk solution to the enzyme, and a possible enzyme deactivation due to unfavorable interactions with the covering layer. For evaluating the enzymatic two-step cascade reaction involving both immobilized enzymes, the same enzymatic activity assay used for the determination of the GOD activity was applied, but without addition of an excess of HRP to the assay solution. Somewhat surprisingly, however, no product formation could be detected. This means that the cascade reaction did not occur if HRP-loaded nanoparticles were coated with the *de*-PG2-BAH-GOD conjugate. This finding might be a consequence of the loss of the reaction intermediate H_2O_2, which is produced in the covering *de*-PG2-BAH-GOD layer and serves as substrate for the second step of the cascade reaction in the subjacent HRP-HMM layer. H_2O_2 may have quickly diffused into the bulk solution and therefore could not reach the HRP molecules within the HMM pores.

Considering this phenomenon, the system containing GOD in the (lower) HMM layer and HRP in the (upper) denpol-BAH-enzyme layer is expected to be more promising to allow an efficient enzymatic cascade reaction, as the reaction intermediate (H_2O_2) is produced in the lower layer and has to diffuse into the bulk solution *via* passing the HRP molecules in the top layer (Scheme 1). This was tested by first coating glass coverslips with the denpol, followed by adsorption of GOD loaded HMM-particles. Analysis of the coverslips coated with *de*-PG2, adsorbed HMM and loaded with GOD showed a GOD activity corresponding to 1.0 pmol GOD/cm^2 (Figure 6a). The storage stability of the layer was monitored by repeated activity measurements upon storing the coverslips with the GOD-HMM layer in pH 7 PBS at 4 °C. Within 14 days, the GOD activity decreased to 40 % of the initial value (Figure 6a).

Comparing the GOD and HRP immobilization within the HMM nanoparticles, the QCM-D measurements showed similar amounts of adsorbed enzyme in both cases, while the activity measurements resulted in a much lower activity in the case of HRP. This indicated unfavorable interactions of HRP with the HMM nanoparticles, resulting in a decreased activity of HRP in the particles

The adsorbed GOD-loaded nanoparticles were then covered with *de*-PG2-BAH-HRP, and a HRP activity of the covering *de*-PG2-BAH-HRP layer corresponding to 8 pmol HRP/cm^2 was measured. For this latter setup, consisting of adsorbed GOD-loaded nanoparticles which were coated with the *de*-PG2-BAH-HRP conjugate, the cascade reaction was measured and found to occur (Figure 6b). This is in clear contrast to the reverse situation where adsorbed HRP-loaded particles were covered with *de*-PG2-BAH-GOD and no activity could be detected at all (see above). As a result of the high HRP loading and the spatial arrangement of the two types of enzymes (GOD in the particles, HRP conjugated to *de*-PG2 on the particles), the cascade reaction was efficiently catalyzed by the immobilized enzymes. The kinetics of the cascade reaction involving both immobilized GOD and HRP was dominated by the GOD activity as addition of HRP in the assay solution did not change the rate of DAP product formation.

Compared to GOD in uncovered nanoparticles (Figure 6a), the GOD activity was reduced from 1.0 pmol GOD/cm^2 to 0.4 pmol GOD/cm^2 by the addition of the covering *de*-PG2-BAH-HRP layer (Figure 6b). At the same time, the addition of the *de*-PG2-BAH-HRP layer resulted in an increased GOD stability (probably due to a lower extent of desorption), retaining about 70-75 % activity after more than 2 weeks (Figure 6b). The prevention of enzyme leaching from mesoporous silica by coating with a polymer has been described previously by Wang and Caruso.[51, 52] Therefore, the covering *de*-PG2-BAH-HRP may not only localize HRP on the nanoparticles but at the same time also prevent GOD leaching from the particles.

Elimination of non-specific GOD binding through a preloading of the mesoporous silica nanoparticles with GOD before immobilization

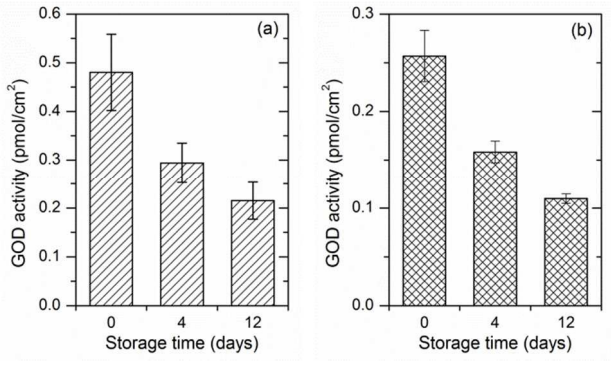

Figure 7. Apparent activity and stability of GOD *preloaded* in HMM particles attached on *de*-PG2-coated glass coverslips (a), and with an additional layer of *de*-PG2-BAH-HRP (b). The latter was measured without additional HRP in the assay mixture; therefore the activity can be assigned completely to the surface localized enzymatic cascade reaction.

As mentioned above, the *in situ* loading of the HMM particles with GOD at pH 5 was accompanied by a considerable non-specific adsorption of GOD to the underlying *de*-PG2 layer. A control experiment without the HMM particles, *i.e.* adsorbing GOD directly on the denpol layer followed by deposition of the top *de*-PG2-BAH-HRP layer resulted in 80 % of the activity in the cascade reaction compared to the samples including HMM particles (data not shown). This confirmed the non-specific GOD binding to the denpol layer. To avoid binding of GOD (pI = 4.2)[50] directly to the denpol layer, the HMM particles were *preloaded* with GOD and after removal of excess GOD the GOD-loaded particles were used for the build-up of the GOD−HMM layer in a single step. This procedure resulted in a GOD activity corresponding to about 0.5 pmol GOD/cm^2 for a surface presenting the GOD-HMM as the top layer (Figure 7a), and 0.25 pmol GOD/cm^2 for the *de*-PG2-BAH-HRP covered GOD-HMM layer (Figure 7b). Therefore, a pre-loading of the HMM particles with GOD and subsequent use of the GOD containing particles for the build-up of the GOD-HMM layer seems to be a promising approach to minimize non-specific adsorption of GOD, thereby making a well-defined cascade reaction in this layered system possible. The GOD stability, however, was lower if compared to the system in which GOD was immobilized on the adsorbed particles (Figure 7b and Fig. 6b).

Conclusions

GOD and HRP were successfully co-immobilized in a layer-by-layer type setup using a polycationic denpol and mesoporous silica nanoparticles. The denpol used in this work, *de*-PG2$_{1400}$, had two different functions. First, coating of a silica surface with the denpol allowed efficient adsorption of the mesoporous silica nanoparticles, in which the first type of enzyme (GOD) was immobilized. Second, the second type of enzyme was added in the form of a denpol-BAH-enzyme conjugate, where the denpol served as a macromolecular scaffold bringing several copies of the second enzyme (HRP) in close proximity to each other and mediating the formation of a stable covering layer on the mesoporous silica nanoparticles (Scheme 1). As a side effect, the presence of the denpol-BAH-HRP layer increased the stability of GOD loaded in the particles (Figure 6), probably due to a prevention of enzyme leaching from the particles. QCM-D was used as a simple and robust measuring technique for the real time study of the step-wise co-immobilization of the two enzymes, and their catalytic activity was measured with suitable enzymatic activity assays.

While the stability of immobilized *de*-PG2-BAH-HRP has previously shown to be high,[28] the storage stability of GOD is a critical issue in this system (Figure 6). For possible applications, the GOD stability may be increased by using other particles, possibly functionalized,[53, 54] which in the past have shown to be excellent hosts for GOD.[55-60]

Whether the general concept of enzyme co-immobilization elaborated in the present work can also be applied to other

enzymatic cascade systems remains to be seen. The proper choice of the mesoporous particle type and pore size is expected to depend on the enzyme of interest. Therefore, experiments for finding the optimal particle system have always to be carried out for achieving optimal performance. Once the optimal mesoporous silica particles are chosen and the denpol-BAH-enzyme conjugate is synthesized, the immobilization procedure for obtaining a spatially controlled enzyme co-immobilization is rather simple, like it is the case for the conventional layer-by-layer deposition methodology.[32, 36]

As a general result, the combination of the two different enzyme immobilization approaches − using HMM nanoparticles as well as denpol-BAH-enzyme conjugates − allows a spatially controlled co-immobilization of different types of enzymes on solid supports. This type of enzyme co-immobilization may find applications in the field of bioelectrode fabrications where a defined localization of redox enzymes is essential for the efficient electron transfer between the immobilized enzymes and the electrode.[61]

Acknowledgements

We would like thank Dr Baozhong Zhang (Polymer Chemistry, Department of Materials, ETH Zürich) for providing us with the dendronized polymer, and Prof. Dr A. Dieter Schlüter (Polymer Chemistry, Department of Materials, ETH Zürich) for constant support.

Author information

[a] Applied Surface Chemistry, Department of Chemical and Biological Engineering, Chalmers University of Technology, SE-412 96 Gothenburg, Sweden
[b] Polymer Chemistry, Department of Materials, ETH Zürich, Vladimir-Prelog-Weg 5, CH-8093 Zürich, Switzerland
[§] Equal contributions.
[*] Corresponding author: *peter.walde@mat.ethz.ch*

Supplementary information

Electronic Supplementary Information (ESI) available: Enzyme activity data, QCM-D results of *de*-PG2 adsorption, SEM images of adsorbed mesoporous silica nanoparticles (HMM). See DOI: 10.1039/b000000x/

References

1. C. Mateo, J. M. Palomo, G. Fernandez-Lorente, J. M. Guisan and R. Fernandez-Lafuente, *Enzyme Microb. Technol.*, 2007, **40**, 1451-1463.
2. S. Hudson, J. Cooney and E. Magner, *Angew. Chem. Int. Ed.*, 2008, **47**, 8582-8594.
3. D. Brady and J. Jordaan, *Biotechnol. Lett.*, 2009, **31**, 1639-1650.
4. R. Fernandez-Lafuente, *Enzyme Microb. Technol.*, 2009, **45**, 405-418.
5. C. Garcia-Galan, Á. Berenguer-Murcia, R. Fernandez-Lafuente and R. C. Rodrigues, *Adv. Synth. Catal.*, 2011, **353**, 2885-2904.
6. D. N. Tran and K. J. Balkus, *ACS Catal.*, 2011, **1**, 956-968.
7. E. Magner, *Chem. Soc. Rev.*, 2013, **42**, 6213-6222.
8. R. A. Sheldon and S. van Pelt, *Chem. Soc. Rev.*, 2013, **42**, 6223-6235.
9. S. Cantone, V. Ferrario, L. Corici, C. Ebert, D. Fattor, P. Spizzo and L. Gardossi, *Chem. Soc. Rev.*, 2013, **42**, 6262-6276.
10. R. DiCosimo, J. McAuliffe, A. J. Poulose and G. Bohlmann, *Chem. Soc. Rev.*, 2013, **42**, 6437-6474.
11. S. Schoffelen and J. C. M. van Hest, *Curr. Opin. Struct. Biol.*, 2013, **23**, 613-621.
12. F. Costantini, R. Tiggelaar, S. Sennato, F. Mura, S. Schlautmann, F. Bordi, H. Gardeniers and C. Manetti, *Analyst*, 2013, **138**, 5019-5024.
13. M. Burchardt and G. Wittstock, *Langmuir*, 2013, **29**, 15090-15099.
14. F. Jia, B. Narasimhan and S. Mallapragada, *Biotechnol. Bioeng.*, 2014, **111**, 209-222.
15. W. Kang, J. Liu, J. Wang, Y. Nie, Z. Guo and J. Xia, *Bioconj. Chem.*, 2014, **25**, 1387-1394.
16. S. F. Mayer, W. Kroutil and K. Faber, *Chem. Soc. Rev.*, 2001, **30**, 332-339.
17. L. Betancor and H. R. Luckarift, *Biotechnol. Genet. Eng. Rev.*, 2010, **27**, 95-114.
18. S.-H. Kim, S.-M. Lee, D.-U. Kim, J.-Z. Cui and S.-W. Kang, *Dyes Pigments*, 2001, **49**, 103-108.
19. H. Gustafsson, E. M. Johansson, A. Barrabino, M. Odén and K. Holmberg, *Colloids Surf., B*, 2012, **100**, 22-30.
20. H. Gustafsson, C. Thörn and K. Holmberg, *Colloids Surf., B*, 2011, **87**, 464-471.
21. C. Thörn, N. Carlsson, H. Gustafsson, K. Holmberg, B. Åkerman and L. Olsson, *Microporous Mesoporous Mater.*, 2013, **165**, 240-246.
22. C. Thörn, H. Gustafsson and L. Olsson, *J. Mol. Catal., B*, 2011, **72**, 57-64.
23. C. Thörn, H. Gustafsson and L. Olsson, *Microporous Mesoporous Mater.*, 2013, **176**, 71-77.
24. C.-H. Lee, T.-S. Lin and C.-Y. Mou, *Nano Today*, 2009, **4**, 165-179.
25. M. Hartmann and D. Jung, *J. Mater. Chem.*, 2010, **20**, 844-857.
26. M. Hartmann and X. Kostrov, *Chem. Soc. Rev.*, 2013, **42**, 6277-6289.
27. N. Carlsson, H. Gustafsson, C. Thörn, L. Olsson, K. Holmberg and B. Åkerman, *Adv. Colloid Interface Sci.*, 2014, **205**, 339-360.
28. A. Küchler, J. Adamcik, R. Mezzenga, A. D. Schlüter and P. Walde, *RSC Adv.*, 2015, **5**, 44530-44544.
29. S. Fornera, T. Bauer, A. D. Schlüter and P. Walde, *J. Mater. Chem.*, 2012, **22**, 502-511.
30. Y. Guo, J. D. van Beek, B. Zhang, M. Colussi, P. Walde, A. Zhang, M. Kröger, A. Halperin and A. D. Schlüter, *J. Am. Chem. Soc.*, 2009, **131**, 11841-11854.
31. A. Grotzky, T. Nauser, H. Erdogan, A. D. Schlüter and P. Walde, *J. Am. Chem. Soc.*, 2012, **134**, 11392-11395.
32. M. Onda, K. Ariga and T. Kunitake, *J. Biosci. Bioeng.*, 1999, **87**, 69-75.
33. P. Pescador, I. Katakis, J. L. Toca-Herrera and E. Donath, *Langmuir*, 2008, **24**, 14108-14114.
34. J. D. Keighron and C. D. Keating, *Langmuir*, 2010, **26**, 18992-19000.
35. S. Guedidi, Y. Yurekli, A. Deratani, P. Déjardin, C. Innocent, S. A. Altinkaya, S. Roudesli and A. Yemenicioglu, *J. Membr. Sci.*, 2010, **365**, 59-67.
36. O. S. Sakr and G. Borchard, *Biomacromolecules*, 2013, **14**, 2117-2135.

37. G. Palazzo, G. Colafemmina, C. Guzzoni Iudice and A. Mallardi, *Sens. Actuators, B*, 2014, **202**, 217-223.
38. B. Solomon, N. Lotan and E. Katchalski-Katzir, *Biopolymers*, 1977, **16**, 1837-1851.
39. B. E. P. Swoboda and V. Massey, *J. Biol. Chem.*, 1965, **240**, 2209-2215.
40. S. Aibara, H. Yamashita, E. Mori, M. Kato and Y. Morita, *J. Biochem.*, 1982, **92**, 531-539.
41. A. B. D. Nandiyanto, S.-G. Kim, F. Iskandar and K. Okuyama, *Micropor. Mesopor. Mat.*, 2009, **120**, 447-453.
42. A. Grotzky, E. Altamura, J. Adamcik, P. Carrara, P. Stano, F. Mavelli, T. Nauser, R. Mezzenga, A. D. Schlüter and P. Walde, *Langmuir*, 2013, **29**, 10831-10840.
43. A. Dirksen and P. E. Dawson, *Bioconj. Chem.*, 2008, **19**, 2543-2548.
44. M. Rodahl, F. Höök, A. Krozer, P. Brzezinski and B. Kasemo, *Rev. Sci. Instrum.*, 1995, **66**, 3924-3930.
45. R. E. Childs and W. G. Bardsley, *Biochem. J.*, 1975, **145**, 93-103.
46. K. C. Brown, J. F. Corbett and N. P. Loveless, *Spectrochim. Acta A*, 1979, **35**, 421-423.
47. S. Fornera and P. Walde, *Anal. Biochem.*, 2010, **407**, 293-295.
48. J. M. Rosenholm and M. Lindén, *Chem. Mater.*, 2007, **19**, 5023-5034.
49. C. B. Lavery, M. C. MacInnis, M. J. MacDonald, J. B. Williams, C. A. Spencer, A. A. Burke, D. J. G. Irwin and G. B. D'Cunha, *J. Agric. Food Chem.*, 2010, **58**, 8471-8476.
50. J. H. Pazur and K. Kleppe, *Biochemistry*, 1964, **3**, 578-583.
51. Y. Wang and F. Caruso, *Chem. Commun.*, 2004, 1528-1529.
52. Y. Wang and F. Caruso, *Chem. Mater.*, 2005, **17**, 953-961.
53. J. Li, G. Yin, Y. Ding, X. Liao, X. Chen, Z. Huang, Y. Yao and X. Pu, *J. Biosci. Bioeng.*, 2013, **116**, 555-561.
54. K. Kandel, S. M. Althaus, M. Pruski, and I. I. Slowing, *ACS Symp. Ser.*, 2013, **1132**, 261-271.
55. X. Zhang, R.-F. Guan, D.-Q. Wu and K.-Y. Chan, *J. Mol. Catal. B: Enzym.*, 2005, **33**, 43-50.
56. D. Lee, J. Lee, J. Kim, J. Kim, H. B. Na, B. Kim, C. H. Shin, J. H. Kwak, A. Dohnalkova, J. W. Grate, T. Hyeon and H. S. Kim, *Adv. Mater.*, 2005, **17**, 2828-2833.
57. C. Lei, Y. Shin, J. K. Magnuson, G. Fryxell, L. L. Lasure, D. C. Elliott, J. Liu and E. J. Ackerman, *Nanotechnol.* 2006, **17**, 5531.
58. Z. H. Dai, J. Ni, X. H. Huang, G. F. Lu and J. C. Bao, *Bioelectrochem.*, 2007, **70**, 250-256.
59. Z. Dai, J. Bao, X. Yang and H. Ju, *Biosens. Bioelectron.*, 2008, **23**, 1070-1076.
60. Z. Zhou and M. Hartmann, *Top. Catal.*, 2012, **55**, 1081-1100.
61. R. A. S. Luz, A. R. Pereira, J. C. P. de Souza, F. C. P. F. Sales and F. N. Crespilho, *ChemElectroChem*, 2014, **1**, 1751-1777.

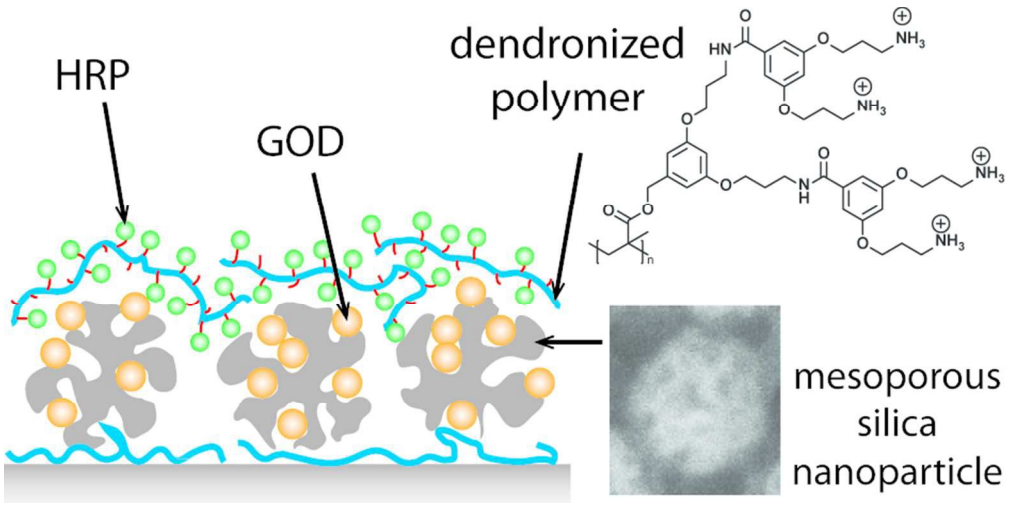

Two enzymes were immobilized in close proximity to each other using enzyme-containing mesoporous nanoparticles and a dendronized polymer-enzyme hybrid structure
79x39mm (300 x 300 DPI)